HEAT TRANSFER CHARACTERISTICS OF MICRO-DROPLET IMPACTING ON HIGH TEMPERATURE WALL IN PYROLYSIS OF METHYL RICINOLEATE

by

Xiaoning MAO[a], Zhendong LIU[a], Liting LI[a], Shangzhi YU[a,b], Qinglong XIE[a,b], Ying DUAN[a], and Yong NIE[a,b*]

[a] Zhejiang Province Key Laboratory of Biofuel,
Biodiesel Laboratory of China Petroleum and Chemical Industry Federation,
College of Chemical Engineering, Zhejiang University of Technology, Hangzhou, Zhejiang, China
[b] State Key Laboratory of Green Chemical Synthesis and Conversion,
Zhejiang University of Technology, Hangzhou, Zhejiang, China

Original scientific paper
https://doi.org/10.2298/TSCI240728247M

The rapid heating of the material is a key factor in the pyrolysis of methyl ricinoleate, which is mainly affected by the droplet size and velocity of methyl ricinoleate droplet impacting on high temperature wall. The process of millimeter-droplet of methyl ricinoleate impacting on high temperature wall at different droplet sizes and velocities were studied by high-speed photography technology and multiphysics simulation. The simulation results were basically consistent with the experimental results. Based on this model, the process of micro-droplet impacting on high temperature wall was investigated, obtaining the heat rates of droplet at different droplet sizes and velocities. The processes of 38~58 μm droplet impacting on high temperature wall at velocity of 10~30 m/s were investigated. As the droplet at the initial temperature of 27 °C and droplet size of 38 μm impacting on a high temperature wall of 480 °C at a speed of 20 m/s, the average heating rate of the droplet reached 10^7 °C per second orders of magnitude. The results showed that faster heating rates were obtained at smaller droplet size and faster droplet velocity. Hence, the rapid heating of the material can be achieved by the micro-droplet impacting on stable high temperature wall.

Key words*: droplet impinging, phase field, micro-droplet, simulation, methyl ricinoleate*

Introduction

Methyl ricinoleate (MR) produced from castor oil can be pyrolyzed at high temperature to form methyl undecylenate (UAME) and heptanal (HEP). The UAME is mainly used to produce polyurethane polymers, cosmetics and pharmaceuticals. Tghe HEP is a chemical intermediate used in the production of spices and cosmetics [1].

In the traditional MR pyrolysis process, the MR diluted with water is preheated and pumped directly into the high temperature electric furnace for pyrolysis [2-4]. In this pyrolysis process, heat is transferred mainly by conduction, which inevitably leads to a temperature gradient from the outer wall of the reactor to the central area of the reactor [5]. This increases the deep pyrolysis and coking of the reactor and thus reduces the yields and selectivities of the products.

* Corresponding author, e-mail: ny_zjut@zjut.edu.cn

In order to solve this problem, our group developed the reactors that utilize microwave assisted heating and induction heating coupled with spray heat transfer for MR pyrolysis [6-8]. During the pyrolysis process, MR is preheated and pumped to the pressure swirl nozzle to break up into microdroplets [9, 10]. Then these droplets hit the high temperature wall at high speed to transfer heat and pyrolyze. The MR droplets can be heated quickly and uniformly [11]. The reaction temperature and heating rate are the key factors in MR pyrolysis [12, 13]. The yields and selectivities of these reactors on the target products are significantly higher than with conventional reactors. Therefore, it is necessary to study the flow and heat transfer properties of MR droplets impacting a high temperature wall. However, direct simulation of spray pyrolysis is impossible due to the detailed hydrodynamic principles such as droplet ejection, droplet interaction with the heated metal surface*, etc.* Hence the modelling currently exceeds the computational power. From the report of Abedinejad *et al.* [14], it is known that when spray-generated droplets evaporate, the collisions between droplets are negligible. Thus, by simulating a single droplet impact without transient consideration of the reaction process, the complexity of the entire spray pyrolysis problem can be reduced and a simplified problem can be simulated numerically [15].

The flow and heat transfer properties of droplets impinging on a high temperature wall are affected by the droplet size, droplet velocity, fluid properties and roughness of the solid wall, which makes the study of the flow and heat transfer properties of droplets impinging on a high temperature wall extreme complicated [16-18]. Currently, the flow and heat transfer properties of droplets impacting a high temperature wall are being studied through experimental research and numerical simulation.

The motion process of droplet impact on a high temperature wall has often been studied using high-speed photography technology. Li *et al.* [19] observed the deposition process of high impacting energy droplets on a horizontal surface by high-speed photography technology. The influence of droplet impacting velocity and size on the impacting process was studied in detail. The results showed that the droplet velocity was the main factor affecting the droplet diffusion during the impacting process. Negeed *et al.* [20] proposed that the droplet impacting velocity, diameter and other parameters will change the contact time of the droplet impacting on the wall. Li *et al.* [21] studied the flow and heat transfer process of droplets impacting on high temperature walls by high-speed photography technology and numerical simulation. The results showed that the heat flux of the droplet is affected by the initial velocity, and the heat transfer efficiency increased with the increasing of the droplet velocity. However, the previous studies mainly focused on the process of low velocity millimeter droplets impacting a high temperature wall, and a simple similarity comparison between large droplets and microdroplets used in establishing previous models is not accurate enough. In addition, there are few studies on the flow and heat transfer properties of microdroplets impacting the high temperature wall.

Numerical simulation provides an efficient way to reveal the heat transfer mechanism of droplet impact. Alhashem *et al.* [22] proposed a model of droplet heat transfer on a vertical plate by combining theory and numerical simulation. For investigate the flow and heat transfer characteristics of micro-droplet impacting on high temperature wall, level-set method, volume of fluid method, Euler-Lagrange method and phase field method were often used to simulate the flow and heat transfer process of droplet impacting [23-25]. In the numerical simulation of the droplet impacting process, it is easier to correctly realize the influence of surface tension and other parameters by using the level set method to track the moving interfaces [26]. The phase-field model used a fixed grid to treat the interface as a thin with limited-size transition layer between different phases [27]. There is no need to use moving meshes to satisfy the ideal-

ized incremental boundary conditions along the interface. In addition, the phase-field approach is highly adaptable and easy to account for thermal coupling effects [28]. However, there are relatively few studies on the simulation of droplet impacting process using a phase field model.

In this study, to simulate the movement and heat transfer process of an MR droplet impacting on a high temperature wall at various particle sizes and velocities, a phase field model was established in this study. This model couples the fluid-flow and heat transfer involved in the single droplet impacting on the high temperature wall. A high-speed camera was employed to record the flow process of a millimeter-droplet of MR impacting on a high temperature wall at a high velocity in order to confirm the accuracy of the model. The simulation results for heat flux were compared with the available experimental data. Then, using this model, the flow and heat transmission properties of the MR micro-droplet impacting on the high temperature wall were examined, and the heating rates of droplet were determined. This work may be useful for refining the atomization procedure in spray pyrolysis.

Experimental

Experimental set up

The experimental set-up was shown in fig. 1, including a tank, a peristaltic pump (BTJ100A, Baoding Guangzhi constant flow pump manufacturing company), a needle (24G, Jiangxi Hongda Medical Devices Group Co., Ltd.), a heating device with glass surface with the roughness is less than 0.05 μm (DB-XWJ, Shanghai Bangxi Lichen Instrument Technology Company), a 100W LED lamp as light source and a high-speed camera (Photron, Fastacm SA-X2, Japan) matching a micro lens (AF micro-Nikkor ED 200 mm f/4 D IF). The peristaltic pump is connected to the needle through a silicone tube, the inner diameter of needle is 0.3 mm, and the high-speed camera is connected to the computer. The high-speed camera lens is parallel to the surface of the heated plate. The temperature error of the top microcrystalline panel (200 mm × 300 mm) can be controlled at ±1 °C.

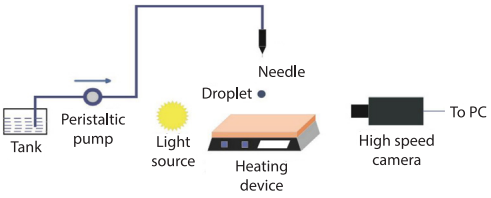

Figure 1. Diagram of experimental device

Experimental procedure

The MR used in the experiment was purified by distillation, and the purity was 98% determined by gas chromatography. First, the glass surface of the heating device was heated to the set temperature (480 °C). The MR was sent to the needle through a peristaltic pump at flow velocity of 6 mL per hour to form a single droplet. Then the droplet was impacted on high temperature wall. The initial temperature of the droplet is room temperature. The impacting velocity of the droplet can be controlled by the distance between the tip and the heated microcrystalline plate, and $t = 0$ seconds was specified as the initial contact time of the droplet on the high temperature wall. The high-speed camera is used to record the impact process of the droplet. In this study, the shooting speed of the high-speed camera is set to 5000 frames per second, which is convenient for quantitative analysis, the pixel of the recorded image is 1024 × 1024. The time interval between two neighboring images is 0.2 ms, the height difference of the droplet on different images and the corresponding time interval can be recorded to calculate the droplet wall speed, the measurement accuracy is ±0.05 m/s. The droplet size and spreading diameter were determined according to the ratio scale. The spreading coefficient, β, was introduced to analyze the spreading degree of droplet, which was expressed:

$$\beta = \frac{l}{D_0} \tag{1}$$

where l [μm] is the spreading diameter of droplet and D_0 [μm] – the initial diameter of droplet.

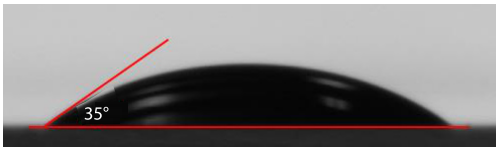

Figure 2. Contact angles of MR on the high temperature wall

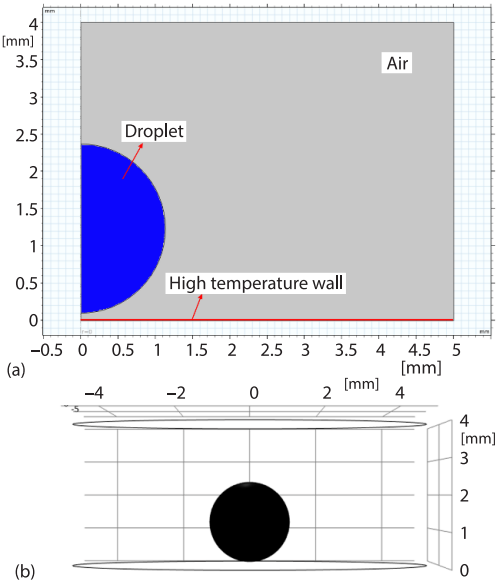

Figure 3. The numerical simulation model of single droplet impacting on high temperature wall; (a) 2-D axisymmetric model and (b) 3-D model

The static contact angle between the MR droplet and the glass surface was measured to be about 35° using the OCA-20 data physics instrument according to the static fixation method as shown in fig. 2. During the experiment, the droplets fall by gravity only. Each set of experiments was repeated three times.

Numerical calculation

Geometric model of droplet impacting on high temperature wall

In the process of MR droplets impacting on high temperature wall, a series of behaviors, such as droplets impingement heat transfer occurrence with high temperature wall, are extremely random and complex. In this paper, the numerical model was built by using the COMSOL Multiphysics software. The simulation was based on the 2-D axisymmetric model established by the experimental results taken by the high-speed camera. The contact angles of MR on high temperature wall inputted in the simulation model were 35°. The geometric model was shown in fig. 3, composed of droplets, high temperature wall and air. The specific values of the initial velocity are obtained experimentally. At the initial moment, the lower end of the MR droplet is in contact with the top of the high temperature wall. As shown in fig. 3(a), the square represented the air and the semicircle represented the droplet. Figure 3(b) was 3-D model by the rotary transform of fig. 3(a). In the related research carried out in this paper, the phase-field coupled heat transfer method will be used to numerically simulate the behavior of MR droplets impinging the high temperature wall, and the heat flux density in the droplet is analyzed. In order to save the simulation cost and speed up the calculation speed, the geometric model of the droplet impacting on high temperature wall was simplified:

– The influence of high temperature wall thermal radiation was ignored.
– The temperature of high temperature wall remained constant.
– The mass remained constant and the reaction process is not considered during the droplet impacting on the high temperature wall.
– The shape of the droplet at the initial time was regular spherical.
– Gas phase air was an ideal gas and the initial air velocity is 0 m/s.
– The fluid was incompressible.

Governing equation

The governing equation of the two-phase flow is a conservation equation based on mass, momentum and energy, which are shown:

$$\rho\left(\frac{\partial\vec{\mathrm{u}}}{\partial t}\right)+\rho\nabla\left(\vec{\mathrm{u}}\vec{\mathrm{u}}\right)=-\nabla P+\nabla\mu\left[\nabla\vec{\mathrm{u}}+\left(\nabla\vec{\mathrm{u}}\right)^{T}\right]+\rho\vec{\mathrm{g}}-\vec{\mathbf{F}}_{\mathrm{st}} \tag{2}$$

$$\nabla\vec{\mathrm{u}}=0 \tag{3}$$

$$\rho\frac{\partial T}{\partial t}+\rho\nabla\left(\vec{\mathrm{u}}T\right)=\nabla\left(\frac{k}{c_p}\nabla\mathrm{T}\right)+Q_e \tag{4}$$

where $\vec{\mathrm{u}}$ is the velocity vector, ρ – the density, P – the pressure, μ – the dynamic viscosity, T – the temperature, $\vec{\mathrm{g}}$ – the gravity vector, $\vec{\mathbf{F}}_{\mathrm{st}}$ – the surface tension per unit volume at the two-phase interface, c_p – the specific heat capacity, k – the thermal conductivity, and Q_e – the source term.

Phase field method is a common method to study interface phenomenon in multi-phase flow. The phase interface between the two-phases can be expressed by the phase field parameter, Φ, which can be described by the Cahn-Hilliard method [29]:

$$\frac{\partial\phi}{\partial t}+\vec{\mathrm{u}}\nabla\phi=\nabla\gamma\nabla G \tag{5}$$

where γ [m^{3}skg^{-1}] is the migration parameters controlling diffusion scale and G [Pa] – the chemical potential at the phase interface.

The formulas for the expressions γ and G are:

$$\gamma=Xe_{pf}^2 \tag{6}$$

$$G=\lambda\left[-\nabla^2\phi+\left[\phi\left(\phi^2-1\right)\right]\exp\left(2\right)\right] \tag{7}$$

where X [mskg^{-1}] is the slip, e_{pf} [m] – the interface liquid film thickness, and λ [N] – the energy mixing density.

The density and dynamic viscosity of the two-phase flow are defined:

$$\rho=\rho_1V_{\mathrm{f}1}+\rho_2V_{\mathrm{f}2} \tag{8}$$

$$\mu=\mu_1V_{\mathrm{f}1}+\mu_2V_{\mathrm{f}2} \tag{9}$$

The subscripts 1 and 2 represent different phases in the formula. The volume fractions V_{f} in two-phases:

$$V_{\mathrm{f}1}=\frac{1-\phi}{2} \tag{10}$$

$$V_{\mathrm{f}2}=\frac{1+\phi}{2} \tag{11}$$

where $\phi=\pm1$ denotes two-phase fluid. The $\phi=0$ represents the phase interface.

The surface tension per unit volume $\vec{\mathbf{F}}_{\mathrm{st}}$ at the interface of the two-phases can be obtained by the gradient of the phase field variable multiplying the chemical potential of the system:

$$\vec{\mathbf{F}}_{\mathrm{st}}=G\nabla\phi \tag{12}$$

Simulation procedure

In previous studies, the Sauter mean diameter of MR after atomization through a pressure swirl nozzle was between 20~70 μm, and the velocity was about 10~30 m/s. Hence, the process of 38 μm, 48 μm, and 58 μm MR droplets impacting on a 480 °C wall at a speed of 10 m/s, 20 m/s, and 30 m/s in 50 μs were simulated by the model. The $t = 0$ seconds was specified as the initial contact time of the droplet impacting on high temperature wall. The spreading coefficient, β, of the droplet in 50 μs was obtained and the average temperature of the droplet was counted by simulating the spreading length of the droplet. Then the heat flux of the high temperature wall was analyzed to investigate the heat transfer process of the droplet impacting on the high temperature wall. For analyzing heat transferring features of on droplet impacting high temperature wall, an accurae estimate of wall heat transfer coefficient is requied. The localized heat flux, q, and the heat flow, Q, at wall were calculated using Fourier's law:

$$q = -k_{\mathrm{f}}\left(\frac{\partial T}{\partial n}\right) = h\left(T_{\mathrm{w}} - T_{\mathrm{f}}\right) \tag{13}$$

$$Q = qA_{\mathrm{f}} \tag{14}$$

The localized heat transfer conefficient of wall is expressed:

$$h = -\frac{k_{\mathrm{f}}}{T_{\mathrm{w}} - T_{\mathrm{f}}}\left(\frac{\partial T}{\partial n}\right) \tag{15}$$

where h is wall heat transfer coefficient, A_{f} – the contact area between fluid and solid, T_{w} – the is temperature of high temperature wall, T_{f} – the fluid temperature, k_{f} – the fluid thermal conductivity, and n – the co-ordinate normal to wall.

Boundary conditions

The upper and right sides of the computational domain were set as pressure boundary conditions in the laminar flow module. The outlet relative pressure is 0 MPa. The bottom side of the computational domain was set to the boundary of the high temperature wall at 480 °C.

The fluid-structure interface follows the basic conservation equations, satisfying the conditions of thermal flux and temperature conservation at the interface of fluid and wall:

$$\begin{aligned} q_{\mathrm{f}} &= q_{\mathrm{w}} \\ T_{\mathrm{f}} &= T_{\mathrm{w}} \end{aligned} \tag{16}$$

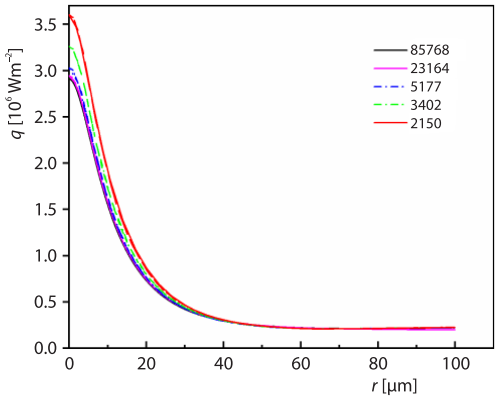

Figure 4. Grid independence verification

Mesh generation

The geometric mesh of the model was divided by the method of physical field control. The model selected the free tetrahedral mesh element. The mesh size was 100 μm × 70 μm. The number of coarsening, conventional, refinement, finer and ultra-fine meshes were 2150, 3402, 5177, 23164, and 85768, respectively. As shown in fig. 4, the mesh size had little effect on simulation results of heat flux at 50 μs. Considering the calculation cost and accuracy, the model used the finer mesh, and the number of grids was 23164.

Results and discussion

Simulation model verification

Simulation of droplet spreading characteristics and experimental verification

Using high-speed photography equipment, the millimeter-scale MR droplet impacting process on the high temperature wall was examined and compared with the outcomes of the simulation. The results as shown in fig. 5. It is evident from the image processing software analysis that the experiment's needle-produced droplets had a diameter of roughly 2 mm. The initial droplet temperature is 23.5 °C. The experimental and simulated droplet spreading diameters achieved their maximums at 4 ms, 7.17 mm and 7.08 mm, respectively, when the droplet struck the wall at a speed of 0.58 m/s. The spreading coefficients in the simulation and the experiment were 3.12 and 3.15, respectively. There was a strong correlation between the experimental and simulated spreading diameters.

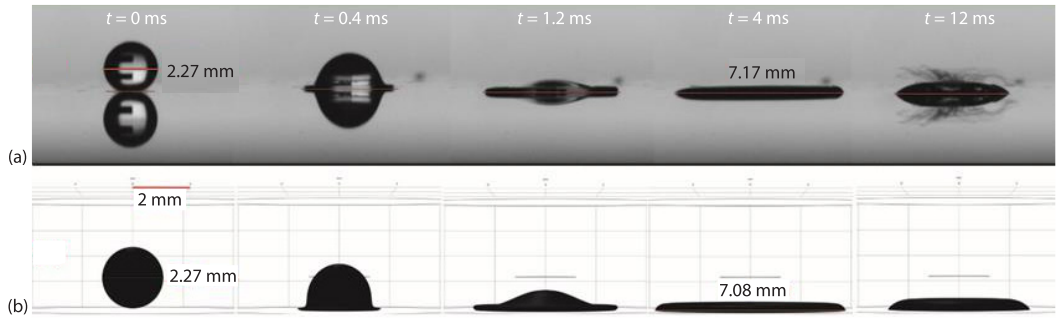

Figure 5. (a) Experimental process and (b) simulation process of MR droplet impacting on high temperature wall

Simulation of heat flux distribution and experimental verification

The millimeter-scale simulation solutions of heat flux and contact temperature at the wall are compared with the available experimental data in order to validate the simulation model. Figure 6 shows the comparison of heat flux variation which was calculated through this model with the experimental date from Moon *et al.* [30] under the condition of a water droplet impacting on the copper wall. The initial droplet diameter is 2 mm, initial impact velocity is 0.5783 m/s, initial droplet temperature is 23.5 °C. It is found that the variation trend of heat flux and the influence trend of temperature predicted by the simulation results are consistent with the experimental data. The deviation between the simulation results and experimental data is tiny at lower initial wall temperature. Therefore, the model can be used to simulate the flow and heat transfer process of droplets impacting on high temperature wall.

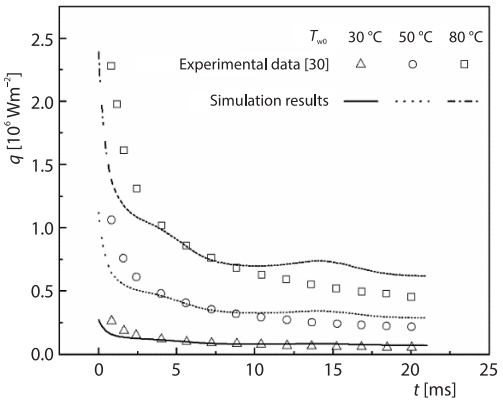

Figure 6. Comparison between simulated and actual heat flux variation

Impact process of micro-droplet on high temperature wall

Effect of droplet size on impact process

The effect of the droplet size on spreading coefficient was presented in fig. 7(a). The micro-droplet can reach the maximum spreading diameter in 10 μs, which was 400 times faster than the millimeter-sized droplets. The variation trend of the spreading coefficient was in good agreement with the experimental results of Visser *et al.* [31]. As the velocity of the droplet was 20 m/s, the spreading coefficient increased with the increasing of droplet size, but the smaller droplet can reach the maximum spreading diameter faster. In addition, the droplets spreading coefficient curve remained basically parallel in the retraction stage, which indicated that the retraction velocity of the droplet was less affected by the droplet size.

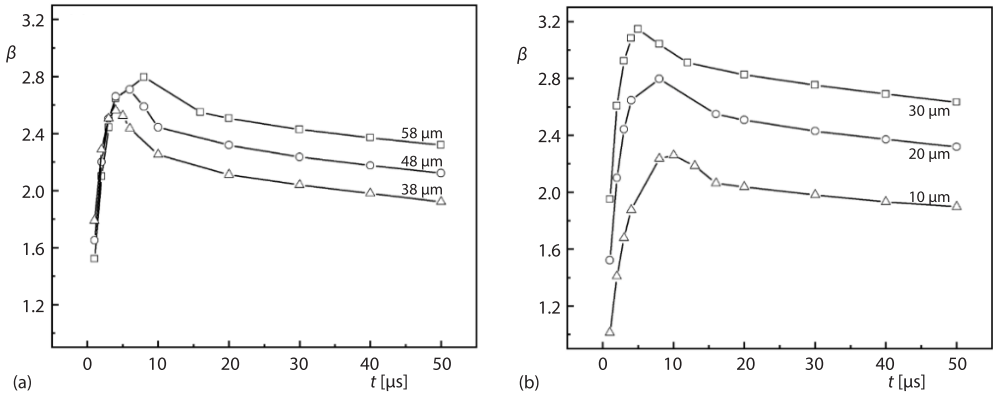

Figure 7. Droplet spreading coefficient, *β*, of; (a) different droplet size and (b) different droplet velocity

Effect of droplet velocity on impact process

As shown in fig. 8, the maximum spreading coefficient of droplet increased with the increasing of droplet velocity. The results was the same as the simulation study of Zhang *et al.* [32]. The effect of the droplet velocity on spreading coefficient was presented in fig. 7(b) when the droplet diameter was 58 μm. The maximum spreading coefficient of the droplet increased with the increasing of the droplet velocity The time required to reach the maximum spreading coefficient decreased with the increasing of the velocity. Droplet of 58 μm reached the maximum spreading diameter in 5 μs at the velocity of 30 m/s, which was half of the time than the droplet of 10 m/s. The spreading coefficient of droplet remained parallel in the retraction stage at different velocity, which indicated that the retraction velocity of the droplet was less affected by the droplet velocity in the droplet impacting on high temperature wall.

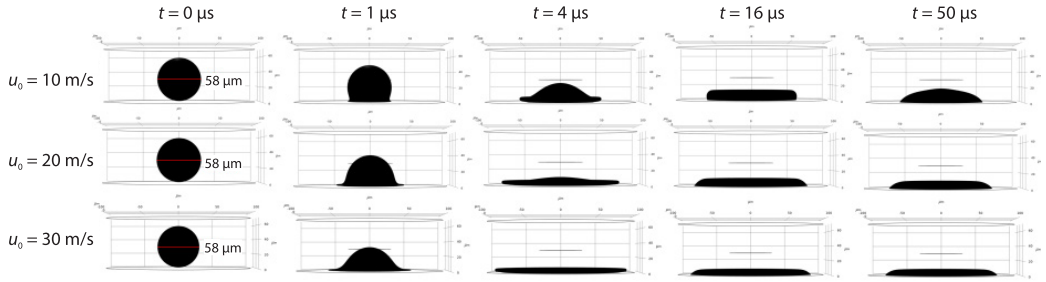

Figure 8. Spreading of droplet impacting on high temperature wall at different droplet velocities

Heat transfer process of micro-droplet on high temperature wall

Heat flux of the wall and temperature distribution of the droplet

The temperature distribution of 58 μm droplet impacting on high temperature wall at a speed of 10 m/s and the average temperature of droplet increased by 117 °C in 1 μs were shown in fig. 9. The high temperature section of the droplet was impacted to the area which was far from the center of the wall by the low temperature section of the droplet in the process of droplet spreading, and the low temperature section of the droplet cannot directly contact with the high temperature wall in the process of droplet retraction. Therefore, the heating rate of the droplet increased with the increasing of the spreading diameter and the decreasing of the time to reach the maximum spreading diameter. During the period of reaching the maximum spreading diameter (0~16 μs), the average heating rates of droplet was $1.8 \cdot 10^7$ °C per second. The average heating rate was obviously higher than the study of Yu *et al.* [11], which was $5.0 \cdot 10^4$ °C per second. This deviation may be caused by the flow process of droplets impingement have been considered in this study. Overall, the spray MR micro-droplet could be flash heated.

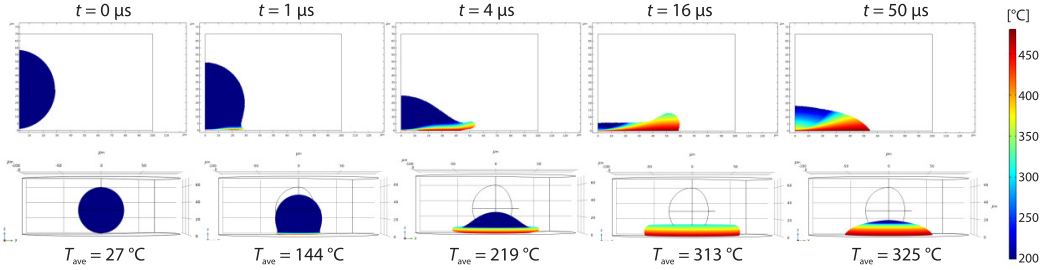

Figure 9. Temperature distribution (58 μm, 10 m/s) of a single droplet impacting on high temperature wall

The radial distribution of high temperature wall heat fluxes at different times were shown in fig. 10. The heat flux was significantly higher than millimeter-droplet impingement [30]. The temperature difference between the high temperature wall and the droplet, and the heat flux decreased with the increasing of the heat transfer time. In addition, the heat flux gradually decreased as the horizontal distance increased. The reason was that the temperature difference between the edge of the droplet and the high temperature wall is small.

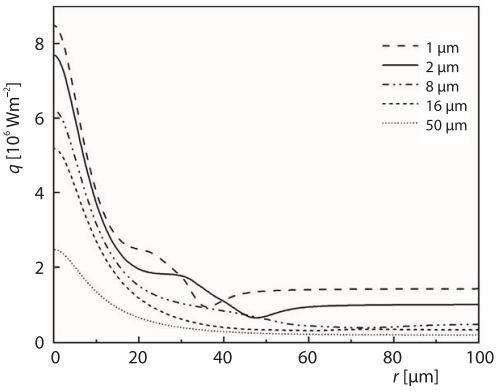

Figure 10. Radial distribution of high temperature wall heat fluxes at different times

Effect of droplet velocity on the heat transfer of the droplet

The heat flux distribution of the droplet impacting on the high temperature wall at the speed of 10 m/s, 20 m/s, and 30 m/s were shown in fig. 11. In fig. 11(a), the differences of heat flux at the radial distance of 20-40 μm in the process of initial impacting were due to the difference in droplet spreading diameter which was caused by different velocity. In addition, droplet will also adhere to the high temperature wall in the initial stage of micro-sized droplet

impacting on high temperature wall. The small temperature difference between the wall and the attachment section of droplet resulted in a low heat flux area. As shown in fig. 11(b), the heat flux decreased with decreasing droplet velocity at the time of 50 μs. The mass and heat transfer processes of the droplet were slow at a low droplet velocity.

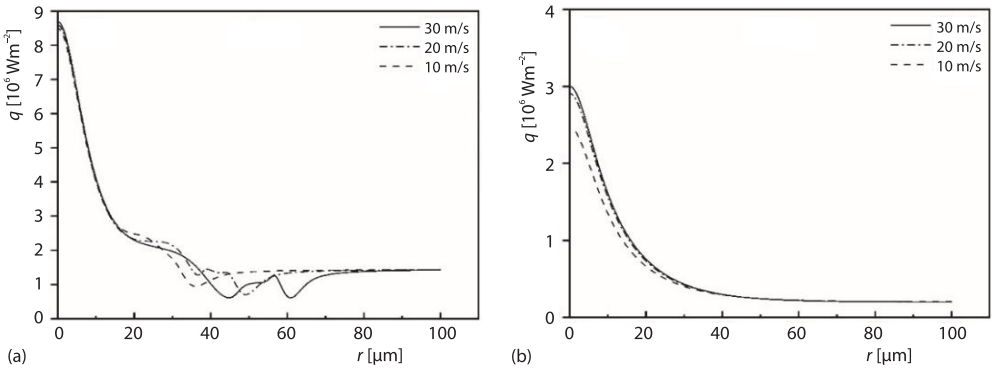

Figure 11. Effect of droplet velocity on the heat flux distributions of high temperature wall at; (a) 1 μs and (b) 50 μs

Effect of droplet size on the heat transfer of the droplet

The effect of droplet size on the distribution of wall heat flux was shown in fig. 12 at the velocity of 20 m/s. As shown in fig. 12(a), owing to the diffusion diameter of the droplet increased with the increasing of the droplet size, the range of wall heat flux increased with the increasing of droplet size at 1 μs. The heat flux in the central area of the high temperature wall was unchanged. This was because the central area of the high temperature wall was still contacted with the low temperature area of the droplet at 1 μs.

As shown in fig. 12(b), the heat flux in the central area of the high temperature wall decreased with the decreasing of droplet size at 50 μs. The temperature difference between the smaller droplet and the high temperature wall was smaller. The reason was that the smaller droplet had a longer contact time with the high temperature wall after reaching the maximum spreading diameter.

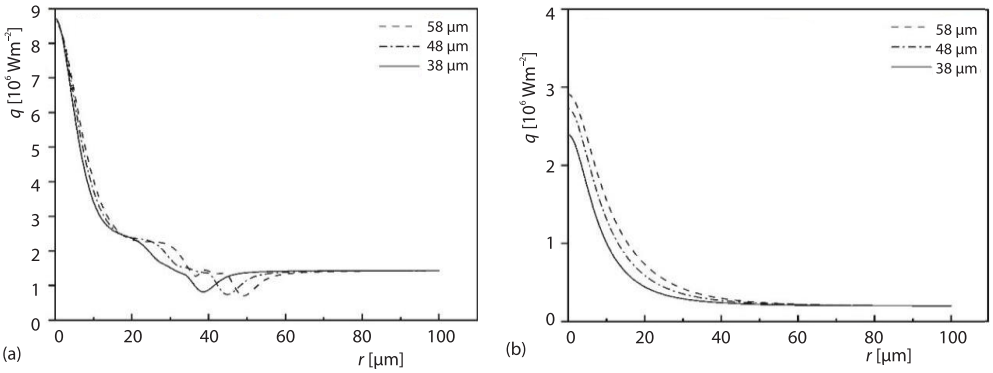

Figure 12. Effect of droplet size on the heat flux distributions of high temperature wall at; (a) 1 μs and (b) 50 μs

Conclusions

In this paper, a phase field model was established to simulate the process of a single droplet impacting on high temperature wall. The process of rapid heating of MR micro-droplet was visualized, and the droplet impacting process was recorded and analyzed to verify the accuracy of the model by high-speed photography technology. The simulation solutions of heat flux were compared with the existing experimental data. Based on this model, the process of micro-droplet impacting on high temperature wall was investigated at different droplet sizes and velocities. The main conclusions were as follows.

- The increase of droplet size will lead to the increase of spreading diameter and the time to reach the maximum spreading diameter. The droplet spreading diameter increased with the increasing of droplet velocity, and the time to reach the maximum spreading diameter was short. The droplet of 58 μm reached the maximum spreading diameter in 5 μs at the velocity of 30 m/s, which was half of the time at the velocity of 10 m/s. The droplet size and velocity had little effect on the droplet retraction speed.
- The droplet with higher velocity can reach the larger maximum spreading diameter in the lower time, and the droplet with smaller size can reach the maximum spreading diameter in the lower time. At the maximum spreading diameter of the droplet, the heating rate increased with the decreasing of droplet size and the increasing of droplet velocity.

The heat transfer rate of the droplet impacting on high temperature wall was on the order of 10^7 °C per second. This showed that the rapid heating of the material can be achieved by the micro-droplet impacting on the stable high temperature wall. Thus, this study could provide reference to the optimization of the atomization process in MR pyrolysis.

Acknowledgment

The authors kindly acknowledge financial support from Zhejiang Province Ten-Thousand Talents Program (Grant No. 2021R52051), National Natural Science Foundation of China (Grant No. 22308329, 21776261).

References

[1] Pereira, E. G., et al., Sustainable Energy: A Review of Gasification Technologies, *Renew. Sustain. Energy Rev.*, *16* (2012), 7, pp. 4753-4762
[2] Han, G., *et al*., Study of Reaction and Kinetics in Pyrolysis of Methyl Ricinoleate, *J. Am. Oil Chem. Soc.*, *73* (1996), 9, pp. 1109-1112
[3] Hu, H. B., *et al.*, Optimization of Production Temperatures of Heptaldehyde and Methyl Undecenoate from Methyl Ricinoleate by Pyrolysis Process, *J. Ind. Eng. Chem.*, *6* (2000), 4, pp. 238-241
[4] Botton, V., *et al*., Thermal Cracking of Methyl Esters in Castor Oil and Production of Heptaldehyde and Methyl Undecenoate, *J. Anal. Appl. Pyrolysis*, *121* (2016), Sept., pp. 387-393
[5] Xu, B., *et al*., Experimental Study on Heat Transfer Characteristics of High-Temperature Heat Pipe, *Thermal Science*, *26* (2022), 6B, pp. 5227-5237
[6] Nie, Y., *et al*., Microwave-Assisted Pyrolysis of Methyl Ricinoleate for Continuous Production of undecylenic Acid Methyl Ester (UAME), *Bioresour. Technol*., *186* (2015), June, pp. 334-337
[7] Mao, X., *et al*., Fast Pyrolysis of Methyl Ricinoleate in an Inductively Heated Reactor Coupled with Atomization Feeding, *Appl. Therm. Eng*., *194* (2021), 2, 117093
[8] Yu, S., *et al*., Pyrolysis of Methyl Ricinoleate by Microwave-Assisted Heating Coupled with Atomization Feeding, *J. Anal. Appl. Pyrolysis*, *135* (2018), 9, pp. 176-183
[9] Yu, S., *et al*., Heat Transfer in a Novel Microwave Heating Device Coupled with Atomization Feeding, *Thermal Science*, *26* (2022), 2A, pp. 1185-1195
[10] Mao, X., *et al*., Predictive Models for Characterizing the Atomization Process in Pyrolysis of Methyl Ricinoleate, *Chinese J. Chem. Eng*., *28* (2020), 4, pp. 1023-1028

[11] Yu, S., *et al*., The 3-D Simulation of a Novel Microwave-Assisted Heating Device for Methyl Ricinoleate Pyrolysis, *Appl. Therm. Eng*., *153* (2019), Mar., pp. 341-351
[12] Mao, X., *et al*., Pyrolysis of Methyl Ricinoleate : Distribution and Characteristics of Fast and Slow Pyrolysis Products, *Materials (Basel)*, *15* (2022), 1565
[13] Liu, H., *et al.*, Thermodynamic Model And Kinetic Compensation Effect of Oil Sludge Pyrolysis Based on Thermogravimetric Analysis, *Thermal Science*, *26* (2022), 1A, pp. 259-272
[14] Abedinejad, M. S., Analysis of Spray Evaporation in a Model Evaporating Chamber: Effect of Air Swirl, *J. Thermal Science*, *32* (2023), 2, pp. 837-853
[15] Silk, E. A., *et al*., Spray Cooling Heat Transfer: Technology Overview and Assessment of Future Challenges for Micro-Gravity Application, *Enenegy Convers. Manag*., *49* (2008), 3, pp. 453-468
[16] Lamini, O., *et al.*, Experimental Study on the Effect of The Liquid/Surface Thermal Properties on Droplet Impact, *Thermal Science*, *25* (2021), 1B, pp. 705-716
[17] Liang, G., Mudawar, I., Review of Drop Impact on Heated Walls, *Int. J. Heat Mass Transf*., *106* (2017), Mar., pp. 103-126
[18] Misyura, S. Y., Morozov, V. S., Droplet Evaporation on a Heated Structured Wall, *Thermal Science*, *23* (2019), 2A, pp. 673-681
[19] Li, J., *et al*., Deposition Process of Droplets Impacting on a Horizontal Surface, *Adv. Mater. Res*., *354-355* (2011), Oct., pp. 579-584
[20] Negeed, E. S. R., *et al*., Dynamic Behavior of Micrometric Single Water Droplets Impacting on Heated Surfaces with TiO_2 Hydrophilic Coating, *Int. J. Therm. Sci.*, *79* (2014), May, pp. 1-17
[21] Li, C., *et al*., A Heat Transfer Model for Aluminum Droplet/Wall Impact, *Aerosp. Sci. Technol.*, *97* (2020), 105639
[22] Alhashem, A., Khan, J., Heat Transfer Analysis for Dropwise-Filmwise Hybrid Surface of Steam on Vertical Plate, *J. Therm. Sci*., *30* (2021), 3, pp. 962-972
[23] Liang, G., *et al.*, Single-Phase Heat Transfer of Multi-Droplet Impact on Liquid Film, *Int. J. Heat Mass Transf*., *132* (2019), Apr., pp. 288-292
[24] Zhang, B., *et al*., Numerical Simulation of Droplet Impinging Icing Process on a Low Temperature Wall with Smoothed Particle Hydrodynamics Method, *Thermal Science*, *26* (2022), 4, pp. 3373-3385
[25] Zhang, R., *et a*l., Analysis of Mist/Air Film Cooling Performance of Trenched Holes with Shaped Lips, *Thermal Science*, *27* (2023), 4, pp. 2639-2649
[26] Tanguy, S., Berlemont, A., Application of a Level Set Method For Simulation of Droplet Collisions, *Int. J. Multiph. Flow*, *31* (2005), 9, pp. 1015-1035
[27] Shen, M., Li, B. Q., A Phase Field Approach to Modelling Heavy Metal Impact in Plasma Spraying, *Coatings*, *12* (2022), 10
[28] Park, Y. J., *et al.*, Adhesion and Rheological Properties of EVA-Based Hot-Melt Adhesives, *Int. J. Adhes. Adhes*., *26* (2006), 8, pp. 571-576
[29] Cahn, J. W., On Spinodal Decomposition, *Acta Metall*., *9* (1961), 9, pp. 795-801
[30] Moon, J. H., *et al.*, Dynamic Wetting and Heat Transfer Characteristics of a Liquid Droplet Impinging on Heated Textured Surfaces, *Int. J. Heat Mass Transf.*, *97* (2016), June, pp. 308-317
[31] Visser, C. W., *et al*., Microdroplet Impact at Very High Velocity, *Soft Matter*, *8* (2012), 41, pp. 10732-10737
[32] Zhang, Z., *et al.*, Numerical Study on Dynamic Behaviours of a Micro-Droplet Impacting on a Vertical Wall In PEMFC, *Int. J. Hydrogen Energy*, *46* (2021), 35, pp. 18557-18570

Paper submitted: July 28, 2024
Paper revised: October 11, 2024
Paper accepted: October 12, 2024

2025 Published by the Vinča Institute of Nuclear Sciences, Belgrade, Serbia.
This is an open access article distributed under the CC BY-NC-ND 4.0 terms and conditions.